Converse magnetoelectric coupling coefficient greater than 10^{-6} s/m in perpendicularly magnetized Co/Pd multilayers on $Pb(Mg_{1/3}Nb_{2/3})O_3$-$PbTiO_3$

T. Usami[a], Y. Sanada[b], Y. Shiratsuchi[c,a,d], S. Yamada[a,b,d], T. Kanashima[b], R. Nakatani[c,a,d], K. Hamaya[a,b,d]

[a] *Center for Spintronics Research Network, Graduate School of Engineering Science, Osaka University, Toyonaka, 560-8531, Osaka, Japan*
[b] *Department of Systems Innovation, Graduate School of Engineering Science, Osaka University, Toyonaka, 560-8531, Osaka, Japan*
[c] *Division of Materials and Manufacturing Science, Graduate School of Engineering, Osaka University, Suita, 565-0871, Osaka, Japan*
[d] *Spintronics Research Network Division, Institute for Open and Transdisciplinary Research Initiatives, Osaka University, Suita, 565-0871, Osaka, Japan*

Abstract

Multiferroic heterostructures consisting of Co/Pd multilayers on $Pb(Mg_{1/3}Nb_{2/3})O_3$-$PbTiO_3$(011) substrates are experimentally investigated. The converse magnetoelectric (CME) effect is characterized by anomalous Hall effect measurements with application of an electric field (E). The remanent magnetization state for the [Co(0.8 nm)/Pd(2 nm)] multilayer is significantly modulated by the application of E. The room-temperature CME coupling coefficient (α_{E}) is estimated to be 1.0-1.1$\times10^{-6}$ s/m, which is the largest among those of multiferroic heterostructures with perpendicular magnetic anisotropy.

Keywords: Magnetoelectric effects, Multiferroic heterostructures, Metastable bcc Co_3Mn, $Pb(Mg_{1/3}Nb_{2/3})O_3$-$PbTiO_3$

1. Introduction

In general, ferroic order parameters of ordinary ferroic materials are controlled by external fields that are conjugate to the order parameters. For

Email addresses: usami.takamasa.es@osaka-u.ac.jp (T. Usami), hamaya.kohei.es@osaka-u.ac.jp (K. Hamaya)

example, magnetisation in ferromagnetic materials and polarisation in ferroelectric ones are tuned by applying a magnetic field (H) and an electric field (E), respectively. On the other hand, in multiferroic materials, more than two ferroic orders simultaneously exist [1, 2], and it leads to magnetoelectric (ME) coupling. The feature enables control of the magnetism by applying E. Until now, much effort has been devoted to obtain large ME coupling because E-control of magnetism has the potential for ultra-low-power data writing in magnetic memory [3, 4, 5, 6, 7, 8], where current-based techniques are traditionally used [9, 10, 11, 12, 13]. Multiferroic materials have been extensively explored for several decades in single-phase multiferroic materials [14, 15, 2]. However, these materials have some obstacles for device applications, e.g., the small number of multiferroic materials, weak ME coupling, and low operation temperature. For that reason, alternative strategies are required to obtain multiferroic materials with a large ME coupling. One of the solutions is to utilize multiferroic heterostructures that consist of ferromagnetic and ferroelectric layers. The multiferroic heterostructures can be operated in a wide range of temperature including room temperature and they show a relativley large ME effect. In addition, they have a variety of material choices. These features are advantageous for device applicatoins compared to single-phase multiferroic materials[16, 17, 18, 19, 20]. Several mechanisms of the ME effect in the multiferroic heterostructures have so far been proposed. In particular, utilization of the strain-mediated ME effect is promising for obtaining a large ME effect [18]. Namely, when E is applied to the ferroelectric layer, the piezoelectric strain is induced, leading to the strain transfer into the ferromagnetic layer though the interface. As a result, the piezostrain deforms the lattice of the ferromagnetic layer, and then, the magnetic properties are efficiently tuned.

To make use of the strain-mediated ME effect, as a ferroelectric layer, we have focused on the $Pb(Mg_{1/3}Nb_{2/3})O_3$-$PbTiO_3$ (PMN-PT). PMN-PT has the largest piezoelectric coefficient [21, 22], which is favorable for the strain-mediated ME effect. Several studies have previously demonstrated a converse ME (CME) effect in multiferroic heterostructures using PMN-PT [23, 24, 25, 26, 27, 28, 29, 30, 31], and CME coupling coefficients (α_{E}) that reach 10^{-5} s/m have been reported very recently [32, 33, 34]. Although these multiferroic heterostructures exhibit a large CME effect, the magnetic layer shows in-plane magnetic anisotropy. The E-control of perpendicular magnetic anisotropy (PMA) is of critical importance for realizing high-density non-volatile memory and logic devices with high thermal stability. Although

several studies have reported the E modulation of PMA in magnetic materials [35, 36, 37, 38, 39, 40, 41], the CME effect is relatively small, and the CME coupling coefficient has remained in the order of 10^{-7} s/m, which is much smaller than that for in-plane magnetic multiferroic heterostructures [35, 36, 41].

Therefore, to achieve a large CME effect in PMA multiferroic heterostructures, we have focused on perpendicularly magnetized Co/Pd multilayers [42, 43, 44, 45, 46]. The origin of PMA in Co/Pd multilayers has been investigated using X-ray magnetic circular dichroism (XMCD) measurements and density functional theory (DFT) calculations [47, 48]. The study revealed that the Co orbital magnetic moments at the Co/Pd interface are anisotropic, and the orbital anisotropy contributes to the emergence of PMA. Therefore, if anisotropic orbital magnetic moments are effectively modulated by the piezostrain of PMN-PT, then a large CME effect would be expected.

In this study, we experimentally investigate multiferroic heterostructures that consist of Co/Pd multilayers on PMN-PT(011). Firstly, we explore the growth of Co/Pd multilayers on the PMN-PT(011) substrates. Polar magneto-optic Kerr effect (MOKE) measurements confirm PMA in the [Co/Pd]/PMN-PT multiferroic heterostructures. In addition, precise control of the magnetic anisotropy from the perpendicular to the in-plane directions is demonstrated by changing the Co thickness (t_{Co}). Anomalous Hall effect measurements indicate that the remanent magnetization state for Co/Pd multilayers with $t_{\mathrm{Co}} = 0.8$ nm is significantly modulated by the application of E. The room-temperature CME coupling coefficient is estimated to be 1.1×10^{-6} s/m, which is the largest among the previously reported PMA multiferroic heterostructures. These results are expected to pave the way for the room-temperature E control of PMA in high-performance spintronic devices.

2. Fabrication of the multiferroic heterostructure

All the Co/Pd multilayers were prepared on 0.5-mm-thick unpolarized PMN-PT substrates. The unpolarized substrates were chosen since the substrates were heated above the ferroelectric Curie temperature of 130°C during the heat treatment of the PMN-PT substrates [49]. The composition of the PMN-PT substrate is $\mathrm{Pb(Mg_{1/3}Nb_{2/3})_{(1-}}_x\mathrm{)O_3\text{-}PbTi}_x\mathrm{O_3}$ ($x = 0.29 - 0.32$), which is close to the morphotropic phase boundary showing the large piezoelectricity. Here, (011) cut substrate is selected because of the relatively

large piezostrain compared to that of the (001) substrate [50, 51, 34], where the maximum piezostrain of ~ 0.3 % with applying an electric field of 0.8 MV/m is expected [34]. The formed multilayer structure is schematically shown in figure 1(a). The growth of the multilayers was performed in an ultra-high-vacuum molecular beam epitaxy (MBE) chamber, and Co and Pd were evaporated with Knudsen cells. The thickness of each layer was determined *in situ* by a thickness monitor using a quartz crystal. Prior to the growth, heat treatment of the PMN-PT substrate was performed at 400°C for 20 min to obtain a flat surface of the PMN-PT(011). The heat-treatment temperature was sufficiently low compared to that in the literature that gives rise to a giant CME effect [32], and we consider degradation of the piezoelectricity due to the heat treatment to be negligible. After cooling the substrate to room temperature, a 3-nm-thick Pd layer was deposited on the substrate, and then a $[\mathrm{Co}(t_{\mathrm{Co}})/\mathrm{Pd}(2\ \mathrm{nm})]_{\times 5}$ multilayer was deposited, where t_{Co} was varied from 0.5 to 1.5 nm. An 8-nm-thick Pd layer was then deposited as a cap layer. During the deposition, the pressure of the chamber was kept under 1×10^{-7} Pa. The deposition rates of Co and Pd were 0.05 and 0.09 Å/sec, respectively.

3. Results

In situ reflection high energy electron diffraction (RHEED) and X-ray diffraction (XRD) measurements were performed for structural characterizations of the [Co/Pd]/PMN-PT heterostructures. Figure 1(b) shows representative RHEED images for the Co/Pd multilayer with t_{Co} =0.5 nm. Clear spot patterns for both Co and Pd layers were observed although weak ring patterns were superimposed. The result indicates that the grown Co/Pd multilayers are highly orientated with some polycrystalline phases.

Figure 1(c) shows the ω-2θ XRD profile for the Co/Pd multilayers with t_{Co} =0.7 nm. A diffraction peak indicated by a black arrow was observed around 40 degrees, and the feature was also seen in the other [Co/Pd]/PMN-PT heterostructures. According to the previous research [46], diffraction peaks for (111) planes from a Pd buffer layer and a Co/Pd multilayer were observed around 40 degrees. Thus, we consider that the present diffraction peak is due to the superposition of diffraction peaks from the (111) planes of the Co/Pd multilayer and the Pd buffer and cap layers. From the RHEED and XRD measurements, it was confirmed that the Co/Pd multilayers are highly (111) orientated even on PMN-PT(011). Magnetic properties of the Co/Pd multi-

layers were characterized by means of polar MOKE measurements at room temperature. Figure 2(a) shows representative polar Kerr hysteresis loops for the Co/Pd multilayers. Rectangular Kerr hysteresis loops with high remanent magnetization states were found for the Co/Pd multilayers with t_{Co} $\leq$ 0.8 nm, indicating the emergence of PMA. As t_{Co} increases, the squareness of the loops decreases and in-plane magnetic anisotropy is gradually observed. Figure 2(b) shows the t_{Co} dependence of the Kerr-rotation angle in the remanent magnetic state ($\theta_{\mathrm{K}}^{\mathrm{rem}}$). Here the angle is normalized with respect to the Kerr-rotation angle in the saturation region. The normalized $\theta_{\mathrm{K}}^{\mathrm{rem}}$ is almost 1 in the range of t_{Co} from 0.5 to 0.7 nm. As t_{Co} increases, $\theta_{\mathrm{K}}^{\mathrm{rem}}$ decreases steeply in the range from 0.7 to 1.0 nm, and then becomes almost 0 at t_{Co}=1.5 nm. The t_{Co} dependence is almost consistent with that previously reported for Co/Pd multilayers on MgO substrates [52]. A recent study revealed that the emergence of the PMA in Co/Pd multilayers is attributed to the anisotropy of the Co orbital magnetic moments [47]. Therefore, the clear t_{Co} dependence in figure 2(b) indicates that the anisotropy of the Co orbital magnetic moments is systematically modulated by changing t_{Co}. This enables us to discuss the correlation between the strain-mediated CME effect and the anisotropy of the Co orbital magnetic moments, discussed in detail later. These results demonstrate the presence of a perpendicularly magnetized Co/Pd multilayer on the PMN-PT(011) substrates, and precise control of the magnetic anisotropy by changing t_{Co}. Here, we focus on multilayers with t_{Co} = 0.7, 0.8, and 0.9 nm because this thickness region is a transition region from PMA to in-plane magnetic anisotropy, which is expected to realize a large CME effect. The saturation magnetization (M_{sat}) of the samples was measured with a vibrating sample magnetometer (VSM) at room temperature. The magnetization curves are shown in figure 2(c). The multilayer with t_{Co} = 0.7 nm shows a rectangular hysteretic shape with a high remanent magnetization. As t_{Co} increases, the remanent magnetization gradually decreases. This trend is consistent with that of the MOKE measurement in figure 2(a). The extracted values of M_{sat} were 1380, 1280, and 1300 kA/m for the multilayers with t_{Co} = 0.7, 0.8, and 0.9 nm, respectively.

To characterize the electric-field effect on the magnetic properties of the Co/Pd multilayers, we adopted the anomalous Hall effect (AHE) measurement with application of E at room temperature, where the method has been established in a previous study of perpendicular FM/FE systems[41]. The setup of the measurement is shown in figure 3(a). A Au (100 nm)/Ti (3 nm) backside electrode is deposited on the bottom of the PMN-PT(011)

substrate, which enables the application of E to the heterostructures along the PMN-PT[011] direction. Prior to the AHE measurement, we first applied an E of -0.8 MV/m. Then, the amplitude of E was gradually changed from -0.8 MV/m to +0.8 MV/m, then back to E=0, which initialized the ferroelectric polarization state. From this zero-electric-field state, E was changed to -0.8 MV/m, and at each step, the AHE signal was obtained as a function of H along the PMN-PT[011]. Here, the Van der Pauw configuration was adopted. To exclude the contributions of magnetoresistance, an even functional component was subtracted from the raw signal, and we treat the subtracted signal as the AHE signal (V_{AHE}).

Figure 3(b) shows the magnetic-field (H) dependence of V_{AHE}, where H was applied along the direction perpendicular to the plane of the film (i.e., PMN-PT[011]). All the samples show hysteretic features, which is consistent with the MOKE measurement. As E is applied, the squareness of the AHE loops decreases for all samples, which indicates the suppression of PMA. In particular, for t_{Co}=0.8 nm, the remanent state is significantly modulated by the application of E.

The E dependence of V_{AHE} is also measured to investigate the E modulation of PMA in detail. Figure 3(c) shows the E dependence of the normalized AHE voltage in the remanent magnetic state ($V_{\mathrm{AHE}}^{\mathrm{rem}}$). The $V_{\mathrm{AHE}}^{\mathrm{rem}}$ is reduced by the application of E, and the PMA is suppressed. We also show the polarization-electric field (P-E) curve of the PMN-PT(011) substrate in the inset of figure 3(c). The polarization reversal occurs around $\pm$0.2 MV/m. This value is close to the point where the suppression of $V_{\mathrm{AHE}}^{\mathrm{rem}}$ starts. Therefore, the change of $V_{\mathrm{AHE}}^{\mathrm{rem}}$ is correlated with the ferroelectric polarization reversal. We discuss the detailed origin of the modulation of $V_{\mathrm{AHE}}^{\mathrm{rem}}$ in the latter section.

From the E dependence of $V_{\mathrm{AHE}}^{\mathrm{rem}}$, we estimate CME coupling coefficient α_{E}, defined as:

$$\alpha_{\mathrm{E}} = \mu_0 \frac{dM_{\mathrm{rem}}}{dE}, \tag{1}$$

where μ_0 is the vacuum permeability. To estimate M_{rem}, it is assumed that the AHE voltage at the saturation region corresponds to M_{sat} measured with the VSM. Based on this assumption, the M_{rem} values are determined as $M_{\mathrm{rem}} = M_{\mathrm{sat}} \times$ (normalized $V_{\mathrm{AHE}}^{\mathrm{rem}}$). As a result, the value of α_{E} is estimated to be 1.0 - 1.1$\times 10^{-6}$ s/m for the heterostructure with $t_{\mathrm{Co}} = 0.8$ nm. As summarized in table 1, the present value is larger than that of Ta/Co/Pt/PMN-PT(011) (9×10^{-7} s/m) which is the largest reported α_{E} among PMA mul-

tiferroic heterostructures [41]. On the other hand, the $\alpha_{\rm E}$ values for $t_{\rm Co}$ = 0.7 and 0.9 nm are 2.1-3.8 $\times 10^{-7}$ and 5.8–8.7 $\times 10^{-7}$, respectively, which are smaller than that for $t_{\rm Co}$=0.8 nm.

Although we performed a similar AHE measurement regarding the positive E, the modulation of the AHE curve was quite small. For in-plane strain curves for PMN-PT(011), asymmetric curves were observed with respect to the polarity of E due to various factors such as flexoelectric effect and internal bias in the PMN-PT(011) [53]. In future work, the origin of the E polarity dependence should be discussed.

In addition to the CME coefficient, we also mention the modulation of the magnetic anisotropy energy. In general, the strain-induced magnetic anisotropy ($K_{\rm u}$) can be written as $K_{\rm u}$=(-3/2)$\lambda\varepsilon E_{\rm Y}/(1-\nu^2)$, where λ is the magnetostriction coefficient, ε is the strain, $E_{\rm Y}$ is Young's modulus, and ν is the Poisson ratio [54]. In our previous study [34], we measured the piezoelectric in-plane strain ε, and it was confirmed that the in-plane compressive strain of about 0.1% was induced along in-plane PMN-PT[100] at E = -0.8 MV/m. Regarding the values of λ, $E_{\rm Y}$, and ν for the Co/Pd multilayer, we took λ=1.5 $\times$ 10^{-4} and $E_{\rm Y}$ = 1.5 $\times$ 10^{11} Pa, based on the literature [55]. We also took ν=0.3 since it is the typical value for metals [54]. As a result, the expected absolute value of $K_{\rm u}$ for applying E = -0.8 MV/m is roughly estimated to be 3.7 $\times$ 10^4 J/m^3. Here, we experimentally found that the application of E suppressed the perpendicular anisotropy of the [Co/Pd]/PMN-PT heterostructure. Therefore, the experimental value of $K_{\rm u}$ can be deduced from the present AHE measurement. As a result, we estimated modulation of the effective perpendicular anisotropy energy from the AHE measurements under E = -0.8 MV/m and E =0, and it was estimated to be 3.7 $\times$ 10^4 J/m^3 for the [Co/Pd] multilayer with $t_{\rm Co}$=0.8 nm. This value is in excellent agreement with the predicted value. This consistent result supports the validity of the present AHE measurement for observing the strain-mediated CME effect.

4. Discussion

The present results raise the question of why a large $\alpha_{\rm E}$ is obtained for the Co/Pd multilayers with $t_{\rm Co}$ = 0.8 nm. To discuss the origin, we consider two possible mechanisms for the variation of the magnetic anisotropy. The first one is a change in the surface anisotropy suggested by Chen *et al* [41]. They reported that the relatively large strain-mediated CME effect in perpendic-

Table 1: Comparison of α_{E} from the present study and those from various PMA multiferroic heterostructures previously reported.

Heterostructure	α_{E} (s/m)	Reference
[Co (0.7 nm)/Pd (2 nm)]$_5$/PMN-PT(011)	2.1–3.8$\times10^{-7}$	This work
[Co (0.8 nm)/Pd (2 nm)]$_5$/PMN-PT(011)	1.0–1.1$\times10^{-6}$	This work
[Co (0.9 nm)/Pd (2 nm)]$_5$/PMN-PT(011)	5.8–8.7$\times10^{-7}$	This work
CoPd alloy (10 nm)/PMN-PT(001)	8.0$\times10^{-7}$	[35]
[Cu (9 nm)/Ni (2 nm)]$_5$/$BaTiO_3$(001)	6$\times10^{-7}$	[36]
Ta (2 nm)/Co (1.85 nm)/Pt (3 nm)/PMN-PT(011)	9$\times10^{-7}$	[41]

ularly magnetized Pt/Co/Ta trilayers on PMN-PT is found via E-induced interface roughening of the Pt/Co/Ta trilayer. However, they also mentioned that inserting a 3-nm-thick Ta layer between the Pt/Co and PMN-PT can suppress the interface roughness caused by the E-induced roughness variation of the substrate. In this study, we have already inserted a 3-nm-thick Pd layer between the Co/Pd multilayer and PMN-PT substrate, inconsistent with the change in the surface anisotropy suggested by Chen *et al* [41]. The another one is an E modification of the orbital magnetic moments. Okabayashi *et al* suggested that the anisotropy of the Co orbital magnetic moment at the Co/Pd interface plays an important role in the emergence of the PMA from angle-dependent XMCD measurements and DFT calculations [47]. Since the Co/Pd multilayers in ref. [47] were (111) orientated, consistent with our present case, the effect of the Co orbital magnetic moment at the Co/Pd interface should be considered. In general, the orbital magnetic moments can be modulated by applying E via the charge accumulation only for a few atomic layers from the dielectric layers [56] or the piezostrain over several hundreds nanometers. In this study, we utilized a sufficiently thick Pd buffer ($\sim$ 3 nm) between the Co/Pd multilayer and the PMN-PT substrate. This means that the charge accumulation in a few atomic layers can be negligible and the piezostrain from the PMN-PT substrate can induce the variation in the orbital magnetic moments.

Next, we further discuss the anisotropy of the Co orbital magnetic moment in our multilayers. The previous study showed that the orbital magnetic moment of Co was anisotropic in the perpendicularly magnetized Co/Pd multilayer, whereas it was isotropic in the in-plane magnetized Co/Pd multilayer [47]. Hence, in our case, it is expected that the Co orbital magnetic moment

is anisotropic in the Co/Pd multilayer with $t_{\mathrm{Co}} = 0.8$ nm, while it is isotropic for $t_{\mathrm{Co}} = 0.9$ nm. From considering this situation and the electric-field dependence of the AHE curve, it is suggested that the anisotropic Co orbital magnetic moment is more sensitive to the piezostrain than the isotropic case; the detailed situation of the multilayer with $t_{\mathrm{Co}} = 0.8$ nm is shown schematically in figure 4. The orbital magnetic moments of Co along the out-of-plane ($m^{\perp}_{\mathrm{orb}}$) and the in-plane ($m^{\parallel}_{\mathrm{orb}}$) directions are depicted as red arrows, and the related Co $3d$ orbitals are shown as blue ellipsoids. The black rectangles indicate the (011) surface of the PMN-PT unit cells. When E is zero, the PMN-PT unit cell is elongated along the PMN-PT[100] direction [34]. In such a situation, the Co $3d(xy,\ x^2 - y^2)$ and $3d(yz,\ zx)$ orbitals that are spread along the in-plane direction are dominantly occupied, since these orbitals become dominant at the Fermi level in the minority-spin state [47]. Therefore, the distribution of the $3d$ electrons shows an oblate pancakelike shape, as shown on the left side of figure 4. This results in an enhancement of $m^{\perp}_{\mathrm{orb}}$ and leads to anisotropy of the Co orbital magnetic moment. On the other hand, when E is applied, the elongated direction changes from the PMN-PT[100] direction to the PMN-PT[01$\bar{1}$] direction, as shown on the right side of figure 4. This suppresses occupation of the Co $3d(xy,\ x^2 - y^2)$ and $3d(yz,\ zx)$ orbitals, and increases that of the $3d\ z^2$ orbital, which leads to the isotropic anisotropy. In other words, the occupation of the Co $3d$ states is modified by the E-induced piezostrain, and it changes the anisotropy of the Co orbital magnetic moments, resulting in variation of the magnetic anisotropy.

In contrast, regarding the in-plane magnetized Co/Pd multilayers with $t_{\mathrm{Co}} = 0.9$ nm, the Co orbital magnetic moment is isotropic, which means that the distribution of the $3d$ electrons at E=0 is isotropic. Therefore, the change of the occupation of the Co $3d$ state is much smaller than that of $t_{\mathrm{Co}} = 0.8$ nm, and it results in the small CME effect. Although the multilayer with $t_{\mathrm{Co}} = 0.7$ nm may also possess anisotropic Co orbital magnetic moments, the CME effect is smaller than that for the multilayer with $t_{\mathrm{Co}} = 0.8$ nm. This is attributed to the PMA being much stronger than the piezostrain-induced anisotropy, so that the CME effect is suppressed more than that with $t_{\mathrm{Co}} = 0.8$ nm. Therefore, the t_{Co} dependence of the CME effect indicates that both the anisotropic Co moment and moderate PMA are important. To confirm the validity of the schematic, a direct estimation of the anisotropic orbital magnetic moments using XMCD under the electric field is needed as discussed in a previous report [40]. In addition, the previous study pointed

out that the magnetic dipole moments (m_{T}) in the Pd atoms also contribute to the emergence of the PMA [47]. In the present schematics, we particularly focus on the Co anisotropic orbital magnetic moments because the value of m_{orb} in Co ($\sim$0.1 μ_{B}) is larger than that of m_{T} in Pd ($\sim$0.01 μ_{B}). However, to clarify the detailed origin of the modulation of the PMA, a further study considering m_{T} in Pd is also required in future work.

5. Conclusions

In summary, we have demonstrated multiferroic heterostructures that consist of PMA Co/Pd multilayers and PMN-PT(011), and a large CME coupling coefficient of 1.0-1.1$\times10^{-6}$ s/m has been achieved for $t_{\mathrm{Co}} = 0.8$ nm at room temperature. This CME coupling coefficient is the largest among those previously reported for multiferroic heterostructures with PMA. The large CME coupling is attributed to both the anisotropic Co orbital magnetic moment and moderate PMA. These results are expected to pave the way for room-temperature E-control of the PMA in high-performance spintronic devices.

Acknowledgments

The authors appreciate Prof. Jun Okabayashi of the University of Tokyo for fruitful discussions. This work was partly supported by Japan Science and Technology Agency (JST) CREST Grant (No. JPMJCR18J1), KAKENHI Grants-in-Aid (No. JP21H05000, JP21K14196, JP22H05000) from the Japan Society for the Promotion of Science (JSPS), and the Spintronics Research Network of Japan (Spin-RNJ).

Declaration of Competing Interest

The authors declare that they have no conflict of interest.

Data Availability

The data that support the findings of this study are available from the corresponding author upon reasonable request.

References

[1] H. Schmid, Multi-ferroic magnetoelectrics, Ferroelectrics 162 (1994) 317–338.

[2] N. A. Spaldin, R. Ramesh, Advances in magnetoelectric multiferroics, Nat. Mater. 18 (2019) 203–212.

[3] J. M. Hu, Z. Li, L. Q. Chen, C. W. Nan, High-density magnetoresistive random access memory operating at ultralow voltage at room temperature, Nat. Commun. 2 (2011) 553.

[4] F. Matsukura, Y. Tokura, H. Ohno, Control of magnetism by electric fields, Nat. Nanotechnol. 10 (2015) 209–220.

[5] S. Bhatti, R. Sbiaa, A. Hirohata, H. Ohno, S. Fukami, S. N. Piramanayagam, Spintronics based random access memory: a review, Materials Today 20 (2017) 530–548.

[6] S. Manipatruni, D. E. Nikonov, C.-C. Lin, T. A. Gosavi, H. Liu, B. Prasad, Y.-L. Huang, E. Bonturim, R. Ramesh, I. A. Young, Scalable energy-efficient magnetoelectric spin–orbit logic, Nature 565 (2019) 35–42.

[7] A. Hirohata, K. Yamada, Y. Nakatani, I.-L. Prejbeanu, B. Diény, P. Pirro, B. Hillebrands, Review on spintronics: Principles and device applications, J. Magn. Magn. Mater. 509 (2020) 166711.

[8] Y. Shiratsuchi, K. Toyoki, R. Nakatani, Magnetoelectric control of antiferromagnetic domain state in Cr_2O3 thin film, J. Phys. Condens. Matter. 33 (2021) 243001.

[9] L. Berger, Emission of spin waves by a magnetic multilayer traversed by a current, Phys. Rev. B 54 (1996) 9353–9358.

[10] J. C. Slonczewski, Current-driven excitation of magnetic multilayers, J. Magn. Magn. Mater. 159 (1996) L1–L7.

[11] I. M. Miron, K. Garello, G. Gaudin, P.-J. Zermatten, M. V. Costache, S. Auffret, S. Bandiera, B. Rodmacq, A. Schuhl, P. Gambardella, Perpendicular switching of a single ferromagnetic layer induced by in-plane current injection, Nature 476 (2011) 189–193.

[12] L. Liu, C.-F. Pai, Y. Li, H. W. Tseng, D. C. Ralph, R. A. Buhrman, Spin-torque switching with the giant spin hall effect of tantalum, Science 336 (2012) 555–558.

[13] A. Hirohata, K. Takanashi, Future perspectives for spintronic devices, J. Phys. D Appl. Phys. 47 (2014) 193001.

[14] N. A. Hill, Why are there so few magnetic ferroelectrics?, The Journal of Physical Chemistry B 104 (2000) 6694–6709.

[15] G. Lawes, G. Srinivasan, Introduction to magnetoelectric coupling and multiferroic films, J. Phys. D Appl. Phys. 44 (2011) 243001.

[16] C.-W. Nan, M. I. Bichurin, S. Dong, D. Viehland, G. Srinivasan, Multiferroic magnetoelectric composites: Historical perspective, status, and future directions, J. Appl. Phys. 103 (2008) 031101.

[17] T. Taniyama, Electric-field control of magnetism via strain transfer across ferromagnetic/ferroelectric interfaces, J. Phys. Condens. Matter. 27 (2015) 504001.

[18] J.-M. Hu, C.-G. Duan, C.-W. Nan, L.-Q. Chen, Understanding and designing magnetoelectric heterostructures guided by computation: progresses, remaining questions, and perspectives, npj Comput. Mater. 3 (2017) 18.

[19] J.-M. Hu, C.-W. Nan, Opportunities and challenges for magnetoelectric devices, APL Mater. 7 (2019) 080905.

[20] S. Yamada, Y. Teramoto, D. Matsumi, D. Kepaptsoglou, I. Azaceta, T. Murata, K. Kudo, V. K. Lazarov, T. Taniyama, K. Hamaya, Electric field tunable anisotropic magnetoresistance effect in an epitaxial $Co_2FeSi/BaTiO_3$ interfacial multiferroic system, Phys. Rev. Mater. 5 (2021) 014412.

[21] S.-E. Park, T. R. Shrout, Ultrahigh strain and piezoelectric behavior in relaxor based ferroelectric single crystals, J. Appl. Phys. 82 (1997) 1804–1811.

[22] Y. Guo, H. Luo, D. Ling, H. Xu, T. He, Z. Yin, The phase transition sequence and the location of the morphotropic phase boundary region in

$(1-x)$[Pb $(Mg_{1/3}$ $Nb_{2/3})O_3$]-xPbTiO_3 single crystal, J. Phys. Condens. Matter. 15 (2003) L77–L82.

[23] T. Wu, A. Bur, P. Zhao, K. P. Mohanchandra, K. Wong, K. L. Wang, C. S. Lynch, G. P. Carman, Giant electric-field-induced reversible and permanent magnetization reorientation on magnetoelectric Ni/(011) $[Pb(Mg_{1/3}Nb_{2/3})O_3]_{(1-x)}$-$[PbTiO_3]_x$ heterostructure, Appl. Phys. Lett. 98 (2011) 012504.

[24] S. Zhang, Y. G. Zhao, P. S. Li, J. J. Yang, S. Rizwan, J. X. Zhang, J. Seidel, T. L. Qu, Y. J. Yang, Z. L. Luo, Q. He, T. Zou, Q. P. Chen, J. W. Wang, L. F. Yang, Y. Sun, Y. Z. Wu, X. Xiao, X. F. Jin, J. Huang, C. Gao, X. F. Han, R. Ramesh, Electric-field control of nonvolatile magnetization in $Co_{40}Fe_{40}B_{20}/Pb(Mg_{1/3}Nb_{2/3})_{0.7}Ti_{0.3}O_3$ structure at room temperature, Phys. Rev. Lett. 108 (2012) 137203.

[25] W. Zhou, C. Ma, Z. Gan, Z. Zhang, X. Wang, W. Tan, D. Wang, Manipulation of anisotropic magnetoresistance and domain configuration in Co/PMN-PT (011) multiferroic heterostructures by electric field, Appl. Phys. Lett. 111 (2017) 052401.

[26] P. Li, Y. Zhao, S. Zhang, A. Chen, D. Li, J. Ma, Y. Liu, D. T. Pierce, J. Unguris, H.-G. Piao, H. Zhang, M. Zhu, X. Zhang, X. Han, M. Pan, C.-W. Nan, Spatially resolved ferroelectric domain-switching-controlled magnetism in $Co_{40}Fe_{40}B_{20}/Pb(Mg_{1/3}Nb_{2/3})_{0.7}Ti_{0.3}O_3$ multiferroic heterostructure, ACS Appl. Mater. Interfaces 9 (2017) 2642–2649.

[27] X. Wang, Q. Yang, L. Wang, Z. Zhou, T. Min, M. Liu, N. X. Sun, E-field control of the RKKY interaction in FeCoB/Ru/FeCoB/PMN-PT (011) multiferroic heterostructures, Adv. Mater. 30 (2018) 1803612.

[28] J. Wang, D. Pesquera, R. Mansell, S. van Dijken, R. P. Cowburn, M. Ghidini, N. D. Mathur, Giant non-volatile magnetoelectric effects via growth anisotropy in $Co_{40}Fe_{40}B_{20}$ films on PMN-PT substrates, Appl. Phys. Lett. 114 (2019) 092401.

[29] Y. Xiang, P. Zhou, Y. Qi, K. Liang, Z. Ma, Y. Liu, Z. Yan, P. Du, R. Xiong, Y. Liu, Z. Xia, M. Popov, D. Filippov, J. Zhang, G. Srinivasan, T. Zhang, Strain and phase transformation co-mediated magnetoelectric

effect in epitaxial Ni/PMN-PT(011) heterostructures, J. Magn. Magn. Mater. 514 (2020) 167138.

[30] T. Usami, S. Fujii, S. Yamada, Y. Shiratsuchi, R. Nakatani, K. Hamaya, Giant magnetoelectric effect in an $L2_1$-ordered $Co_2FeSi/Pb(Mg_{1/3}Nb_{2/3})O_3$-$PbTiO_3$ multiferroic heterostructure, Appl. Phys. Lett. 118 (2021) 142402.

[31] L. Leiva, J. L. Ampuero Torres, J. E. Gómez, D. Velázquez Rodriguez, J. Milano, A. Butera, Electric field control of magnetism in FePt/PMN-PT heterostructures, J. Magn. Magn. Mater. 544 (2022) 168619.

[32] A. Begue, M. Ciria, Strain-mediated giant magnetoelectric coupling in a crystalline multiferroic heterostructure, ACS Appl. Mater. Interfaces 13 (2021) 6778–6784.

[33] P. B. Meisenheimer, R. A. Steinhardt, S. H. Sung, L. D. Williams, S. Zhuang, M. E. Nowakowski, S. Novakov, M. M. Torunbalci, B. Prasad, C. J. Zollner, Z. Wang, N. M. Dawley, J. Schubert, A. H. Hunter, S. Manipatruni, D. E. Nikonov, I. A. Young, L. Q. Chen, J. Bokor, S. A. Bhave, R. Ramesh, J. M. Hu, E. Kioupakis, R. Hovden, D. G. Schlom, J. T. Heron, Engineering new limits to magnetostriction through metastability in iron-gallium alloys, Nat. Commun. 12 (2021) 2757.

[34] S. Fujii, T. Usami, Y. Shiratsuchi, A. M. Kerrigan, A. M. Yatmeidhy, S. Yamada, T. Kanashima, R. Nakatani, V. K. Lazarov, T. Oguchi, Y. Gohda, K. Hamaya, Giant converse magnetoelectric effect in a multiferroic heterostructure with polycrystalline Co_2FeSi, NPG Asia Mater. 14 (2022) 43.

[35] J.-H. Kim, K.-S. Ryu, J.-W. Jeong, S.-C. Shin, Large converse magnetoelectric coupling effect at room temperature in CoPd/PMN-PT (001) heterostructure, Appl. Phys. Lett. 97 (2010) 252508.

[36] Y. Shirahata, R. Shiina, D. L. González, K. J. A. Franke, E. Wada, M. Itoh, N. A. Pertsev, S. van Dijken, T. Taniyama, Electric-field switching of perpendicularly magnetized multilayers, NPG Asia Mater. 7 (2015) e198–e198.

[37] Y. Sun, Y. Ba, A. Chen, W. He, W. Wang, X. Zheng, L. Zou, Y. Zhang, Q. Yang, L. Yan, C. Feng, Q. Zhang, J. Cai, W. Wu, M. Liu, L. Gu,

Z. Cheng, C.-W. Nan, Z. Qiu, Y. Wu, J. Li, Y. Zhao, Electric-field modulation of interface magnetic anisotropy and spin reorientation transition in $(Co/Pt)_3$/PMN-PT heterostructure, ACS Appl. Mater. Interfaces 9 (2017) 10855–10864.

[38] B. Peng, Z. Zhou, T. Nan, G. Dong, M. Feng, Q. Yang, X. Wang, S. Zhao, D. Xian, Z.-D. Jiang, W. Ren, Z.-G. Ye, N. X. Sun, M. Liu, Deterministic Switching of Perpendicular Magnetic Anisotropy by Voltage Control of Spin Reorientation Transition in $(Co/Pt)_3/Pb(Mg_{1/3}Nb_{2/3})O_3$-$PbTiO_3$ Multiferroic Heterostructures, ACS Nano 11 (2017) 4337–4345.

[39] Q. Yang, T. Nan, Y. Zhang, Z. Zhou, B. Peng, W. Ren, Z.-G. Ye, N. X. Sun, M. Liu, Voltage Control of Perpendicular Magnetic Anisotropy in Multiferroic $(Co/Pt)_3/PbMg_{1/3}Nb_{2/3}O_3$-$PbTiO_3$ Heterostructures, Phys. Rev. Appl. 8 (2017) 044006.

[40] J. Okabayashi, Y. Miura, T. Taniyama, Strain-induced reversible manipulation of orbital magnetic moments in ni/cu multilayers on ferroelectric $batio_3$, npj Quantum Mater 4 (2019) 21.

[41] A. Chen, H. Huang, Y. Wen, W. Liu, S. Zhang, J. Kosel, W. Sun, Y. Zhao, Y. Lu, X.-X. Zhang, Giant magnetoelectric effect in perpendicularly magnetized Pt/Co/Ta ultrathin films on a ferroelectric substrate, Materials Horizons 7 (2020) 2328–2335.

[42] P. F. Carcia, A. D. Meinhaldt, A. Suna, Perpendicular magnetic anisotropy in Pd/Co thin film layered structures, Appl. Phys. Lett. 47 (1985) 178–180.

[43] B. M. Lairson, J. Perez, C. Baldwin, Application of Pd/Co multilayers for perpendicular magnetic recording, Appl. Phys. Lett. 64 (1994) 2891–2893.

[44] M. T. Johnson, P. J. H. Bloemen, F. J. A. d. Broeder, J. J. d. Vries, Magnetic anisotropy in metallic multilayers, Rep. Prog. Phys. 59 (1996) 1409.

[45] Y. Fu, S. Ishio, T. Wang, W. Pei, T. Hasegawa, H. Yamane, H. Saito, Tuning interlayer coupling and domain structure in

$[Co/Pd]_nCo/Ru[Co/Pd(x)]_m$ multilayer by controlling the thickness x of the weak-ferromagnetic Pd layers in the lower Co/Pd multilayer, J. Appl. Phys. 105 (2009) 07C307.

[46] C. W. Barton, T. J. A. Slater, R. M. Rowan-Robinson, S. J. Haigh, D. Atkinson, T. Thomson, Precise control of interface anisotropy during deposition of Co/Pd multilayers, J. Appl. Phys. 116 (2014) 203903.

[47] J. Okabayashi, Y. Miura, H. Munekata, Anatomy of interfacial spin-orbit coupling in Co/Pd multilayers using x-ray magnetic circular dichroism and first-principles calculations, Sci. Rep. 8 (2018) 8303.

[48] Y. Miura, J. Okabayashi, Understanding magnetocrystalline anisotropy based on orbital and quadrupole moments, J. Phys.: Condens. Matter 34 (2022) 473001.

[49] B. Noheda, D.E. Cox, G. Shirane, J. Gao, Z.G. Ye, Phase diagram of the ferroelectric relaxor (1-x)$PbMg_{1/3}Nb_{2/3}O_{3-x}$-$PbTiO_3$, Phys. Rev. B 66 (2002) 054104.

[50] L. Yang, Y. Zhao, S. Zhang, P. Li, Y. Gao, Y. Yang, H. Huang, P. Miao, Y. Liu, A. Chen, C. W. Nan, C. Gao, Bipolar loop-like non-volatile strain in the (001)-oriented $Pb(Mg_{1/3}Nb_{2/3})O_3$-$PbTiO_3$ single crystals, Sci. Rep. 4 (2014) 4591.

[51] T. Usami, S. Fujii, S. Yamada, Y. Shiratsuchi, T. Kanashima, R. Nakatani, K. Hamaya, Converse Magnetoelectric Effect in Epitaxial Co_2MnSi/$Pb(Mg_{1/3}Nb_{2/3})O_3$-$PbTiO_3$ Multiferroic Heterostructures, IEEE Trans. Magn. 58 (2022) 1–5.

[52] K. Tobari, M. Ohtake, K. Nagano, M. Futamoto, Influence of layer thickness on the structure and the magnetic properties of Co/Pd epitaxial multilayer films, J. Magn. Magn. Mater. 324 (2012) 1059–1062.

[53] W. Hou, S. A. Chowdhury, A. Dey, C. Watson, T. Peña, A. Azizimanesh, H. Askari, S. M. Wu, Nonvolatile ferroelastic strain from flexoelectric internal bias engineering, Phys. Rev. Appl. 17 (2022) 024013.

[54] N. Lei, S. Park, P. Lecoeur, D. Ravelosona, C. Chappert, O. Stelmakhovych, V. Holý, Magnetization reversal assisted by the inverse

piezoelectric effect in Co-Fe-B/ferroelectric multilayers, Phys. Rev. B 84 (2011) 012404.

[55] N. Sato, Crystallographic structure and magnetism of Co - Pd and Co - Pt films with an artificially layered structure, J. Appl. Phys. 64 (1988) 6424–6433.

[56] S. Miwa, M. Suzuki, M. Tsujikawa, T. Nozaki, T. Nakamura, M. Shirai, S. Yuasa, Y. Suzuki, Perpendicular magnetic anisotropy and its electric-field-induced change at metal-dielectric interfaces, J. Phys. D Appl. Phys. 52 (2019) 063001.

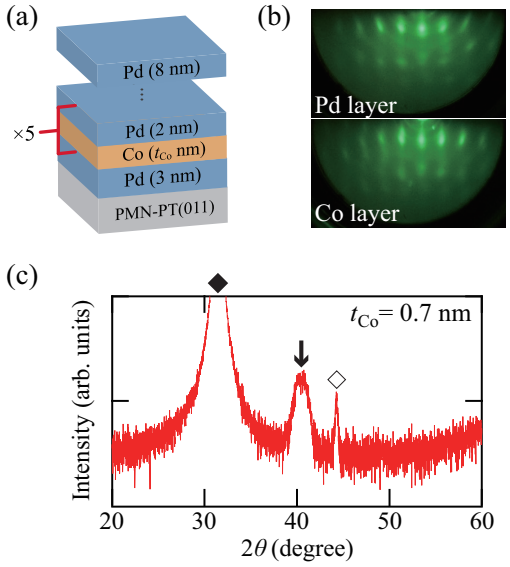

Figure 1: (a) Schematic of the [Co/Pd]/PMN-PT multiferroic heterostructure. (b) Representative RHEED images for the Co/Pd multilayers with $t_{\mathrm{Co}} = 5$ nm. (c) XRD profile for the [Co/Pd]/PMN-PT multiferroic heterostructure with t_{Co} =0.7 nm. Black arrows indicate a diffraction peak from the (111) planes of the Co/Pd multilayer and the Pd buffer and cap layers. The peaks indicated by the solid and open squares originate from the (011) plane of the PMN-PT and an artifactual factor, respectively.

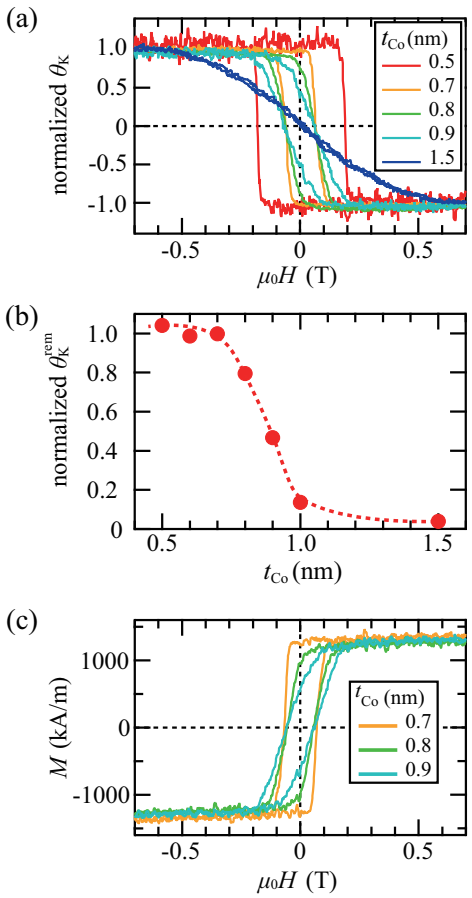

Figure 2: (a) Representative polar Kerr hysteresis loops of the Co/Pd multilayers at room temperature. The Kerr-rotation angle (θ_K) was normalized with respect to that in the saturation region. (b) Dependence of the normalized remanent Kerr-rotation angle on the Co-thickness. (c) Magnetization curves of the Co/Pd multilayers with t_{Co} = 0.7, 0.8, and 0.9 nm at room temperature.

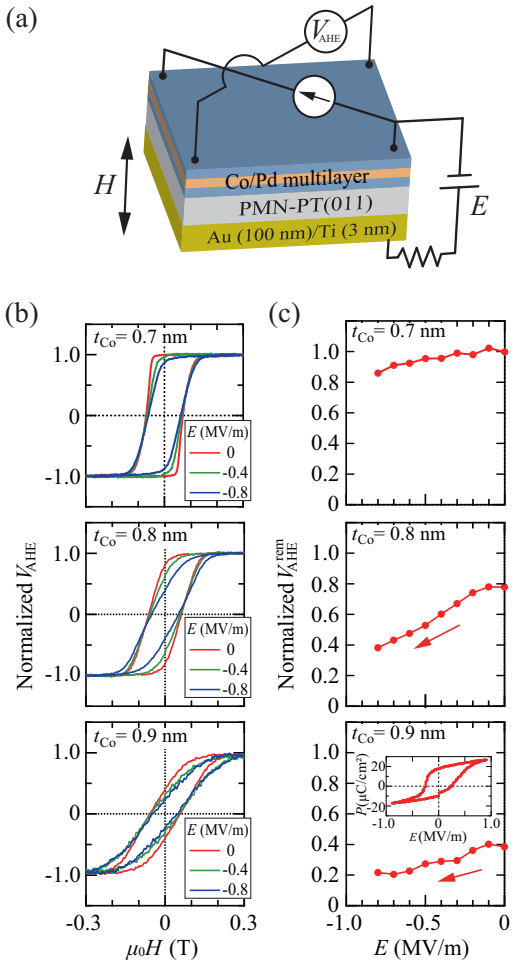

Figure 3: (a) Schematic of the configuration for measurement of the anomalous Hall effect (AHE) with application of E. (b) Normalized AHE curves for the [Co/Pd]/PMN-PT multiferroic heterostructures with t_{Co} =0.7, 0.8, and 0.9 nm under various E at room temperature. (c) Electric-field dependence of the normalized remanent state of the [Co/Pd]/PMN-PT multiferroic heterostructures with t_{Co} =0.7, 0.8, and 0.9 nm at room temperature. The inset is the polarization-electric field (P-E) curve of the PMN-PT (011) substrate at room temperature.

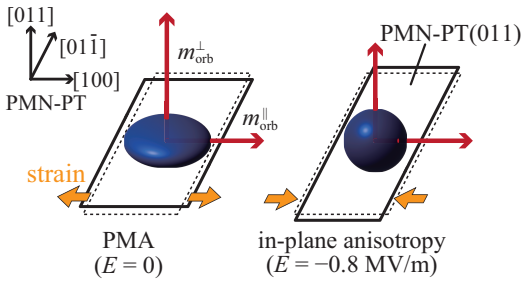

Figure 4: Schematic diagrams of the orbital magnetic moments (red arrows) and the related distributions of the Co d orbitals (blue ellipsoid) in the multilayer with $t_{\mathrm{Co}} = 0.8$ nm. The rectangles indicate the (011) surface of the PMN-PT unit cells. The dashed lines indicate the pristine unpoled ferroelectric state of PMN-PT(011).